APL Materials

How much gallium do we need for a p-type $Cu(In,Ga)Se_2$?

Cite as: APL Mater. **10**, 061108 (2022); https://doi.org/10.1063/5.0091676
Submitted: 16 March 2022 • Accepted: 23 May 2022 • Published Online: 17 June 2022

Omar Ramírez, Evandro Martin Lanzoni, Ricardo G. Poeira, et al.

ARTICLES YOU MAY BE INTERESTED IN

An improved acoustic imaging algorithm combining object detection and beamforming for acoustic camera
JASA Express Letters **2**, 064802 (2022); https://doi.org/10.1121/10.0011735

Ultraviolet nanosecond laser ablation of polyimide with thermal and nonthermal effects near threshold fluence
Journal of Laser Applications **34**, 032004 (2022); https://doi.org/10.2351/7.0000674

Preface: 2021 Asia-Pacific Conference on Applied Mathematics and Statistics
AIP Conference Proceedings **2471**, 010001 (2022); https://doi.org/10.1063/12.0009180

© 2022 Author(s).

How much gallium do we need for a p-type $Cu(In,Ga)Se_2$?

Cite as: APL Mater. 10, 061108 (2022); doi: 10.1063/5.0091676
Submitted: 16 March 2022 • Accepted: 23 May 2022 •
Published Online: 17 June 2022

View Online

Export Citation
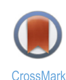
CrossMark

Omar Ramírez,[1,a] Evandro Martin Lanzoni,[1] Ricardo G. Poeira,[1] Thomas P. Weiss,[1] Renaud Leturcq,[2] Alex Redinger,[1] and Susanne Siebentritt[1]

AFFILIATIONS

[1] Department of Physics and Materials Science, University of Luxembourg, 41 rue du Brill, Belvaux L-4422, Luxembourg
[2] Materials Research and Technology Department, Luxembourg Institute of Science and Technology, 41 rue du Brill, Belvaux L-4422, Luxembourg

[a] Author to whom correspondence should be addressed: omar.ramirez@uni.lu

ABSTRACT

Doping in the chalcopyrite $Cu(In,Ga)Se_2$ is determined by intrinsic point defects. In the ternary $CuInSe_2$, both N-type conductivity and P-type conductivity can be obtained depending on the growth conditions and stoichiometry: N-type is obtained when grown Cu-poor, Se-poor, and alkali-free. $CuGaSe_2$, on the other hand, is found to be always a P-type semiconductor that seems to resist all kinds of N-type doping, no matter whether it comes from native defects or extrinsic impurities. In this work, we study the N-to-P transition in Cu-poor $Cu(In,Ga)Se_2$ single crystals in dependence of the gallium content. Our results show that $Cu(In,Ga)Se_2$ can still be grown as an N-type semiconductor until the gallium content reaches the critical concentration of 15%–19%, where the N-to-P transition occurs. Furthermore, trends in the Seebeck coefficient and activation energies extracted from temperature-dependent conductivity measurements demonstrate that the carrier concentration drops by around two orders of magnitude near the transition concentration. Our proposed model explains the N-to-P transition based on the differences in formation energies of donor and acceptor defects caused by the addition of gallium.

© 2022 Author(s). All article content, except where otherwise noted, is licensed under a Creative Commons Attribution (CC BY) license (http://creativecommons.org/licenses/by/4.0/). https://doi.org/10.1063/5.0091676

I. INTRODUCTION

Despite sharing a similar electronic structure, one of the most puzzling differences between $CuInSe_2$ and $CuGaSe_2$ is the fact that the former can be intrinsically doped N or P-type, while the latter is always a P-type semiconductor regardless of the growth conditions or deviations from molecularity and valence stoichiometry.[1] In the ternary $CuInSe_2$, there are three main parameters involved in determining its conductivity type: (I) the overall copper content,[2] (II) the selenium pressure during or after growth,[3] and (III) the presence of alkali metals.[4,5] In order to achieve N-type $CuInSe_2$, the sample must be alkali-free, have been grown under low Se pressure, and be either Cu-poor or close-to-stoichiometric.[2,6] Each of these conditions on its own has the capability to change the conductivity type from N to P, i.e., having a Cu-rich composition, adding alkali metals either through a postdeposition treatment or from the soda lime glass,[4] or annealing under a high selenium pressure,[3] would result in a P-type $CuInSe_2$. Single crystals grown by metalorganic vapor phase epitaxy (MOVPE) comply with all three conditions to obtain N-type conductivity. As the selenium overpressure in MOVPE is considerably lower than in a co-evaporation,[7] and the fact that selenium cannot be supplied during the cool down stage, it has been shown that alkali-free $CuInSe_2$ single crystals grown by MOPVE are always N-type regardless of the Se partial pressure used during growth as long as the composition is Cu-poor.[4]

In the case of $CuGaSe_2$, Zunger *et al.* have performed extensive theoretical studies on the possibility to achieve N-type doping by extrinsic impurities, such as H, Cd, Zn, Mg, Cl, and other halogens[8–10] and found that none of them can effectively produce an N-type behavior. A more recent theoretical study on Zn-doped $CuGaSe_2$ suggested that N-type behavior could only be achieved if Zn would substitute copper sites, as the partial or total occupation of gallium sites by Zn would result in a P-type material.[11] In the case of H-doped $CuGaSe_2$, Han *et al.* concluded that only the incorporation of H from an atomic source like a hydrogen plasma treatment could invert the conductivity from P to N-type.[12] Experimentally, group IV elements, such as Ge[13] and Si,[14] have been used in attempts to dope $CuGaSe_2$ N-type. In both cases, the dopants

© Author(s) 2022

were found to create donor states that involve donor–acceptor pair recombination; however, the bulk conductivity remained P-type.[15] The fact that $CuGaSe_2$ resists N-type doping has been pointed out as a part of a general trend in semiconductor families, where the wider-bandgap member exists often in only one doping type, like AlN when compared to GaN and InN, due to the so-called "doping limit rule."[9,16]

The fact that $CuInSe_2$ can be grown as an N-type semiconductor under Cu-poor conditions and that $CuGaSe_2$ is always P-type, indicates that within Cu-poor $Cu(In,Ga)Se_2$ exists a transition point caused by the alloy with gallium. The aim of this work is to provide experimental evidence of such a transition and to understand the reasons for the change in the type of majority carriers. In order to carry out this investigation, several $Cu(In,Ga)Se_2$ single crystals of around 530 nm thickness were grown by metalorganic vapor phase epitaxy (MOVPE). Since the presence of alkalis and the Cu-content plays a crucial role in determining the conductivity type, the copper content of all the $Cu_y(In,Ga)Se_2$ single crystals was restricted to $0.8 < y < 0.9$, while the presence of alkalis was suppressed by using undoped GaAs wafers as a substrate.

II. METHODS

The $CuIn_{1-x}Ga_xSe_2$ single crystals used in these experiments were grown by metalorganic vapor phase epitaxy (MOVPE) on semi-insulating 500 μm thick (100)-oriented GaAs 2 in. epi-ready wafers at 520 °C and 90 mbar. A two-step growth process was implemented in order to finely tune the gallium content. After growth, the samples remained in an N_2-filled glove box. All characterization techniques were carried out on bare absorbers freshly cleaved from the wafer. Details of the heteroepitaxial growth, cross section scanning electron microscopy images, and a secondary-ion mass spectrometry analysis of selected samples can be found in Sec. S1 of the supplementary material.

Photoluminescence spectra were obtained by exciting bare absorbers with a 660 nm diode laser and collecting the emitted photoluminescence into an InGaAs array spectrometer. All measurements were performed at room temperature and spectrally corrected using a calibrated halogen lamp.

Temperature-dependent conductivity measurements were performed in a closed-cycle cryostat. Samples of 0.6 × 0.6 mm^2 were prepared in the Van der Pauw configuration by evaporating triangular gold contacts with a thickness of 150 nm. For the Seebeck coefficient measurements, rectangular pieces of each sample were cleaved and mechanically pressed onto a home-made setup consisting of two copper pieces (one thermalized at room temperature and one heated). Details of the setup can be found elsewhere.[17]

Energy-dispersive x-ray spectroscopy was carried out at 5 kV, and the L-line of all elements was used for quantification. No traces of arsenic were detected at this acceleration voltage, ensuring that the gallium atomic percentage measured was not affected by the GaAs substrate.

XPS measurements were carried out using a hemispherical energy analyzer from Prevac (EA15) with a 2d detection system MCP/camera detector. The energy analyzer is assembled in the UHV analysis chamber from Scienta Omicron. A Kα x-ray source with a photon energy of 1486.6 eV was used in these measurements. The survey spectra were collected using a straight slit 2.5 × 25 mm^2, pass energy of 200 eV, and energy step of 0.192 eV. The samples were mounted in the same sample holder using the same ground connection and then transferred without air exposure from a glovebox to the UHV XPS chamber under an inert gas transfer system.

III. RESULTS AND DISCUSSION

Since the determination of the gallium content was of utmost importance for the purpose of this investigation, different techniques were used to measure the percentage of Ga present in each sample. Since an increase in the bandgap due to the shift of the conduction band (CB) is expected for higher gallium contents,[18,19] it is possible to approximate the Ga concentration from the optical bandgap dictated by the position of the maximum of the photoluminescence (PL) spectrum and the experimentally determined expression: $E_g = 1.01 + 0.626x - 0.167x(1 - x)$, where x is the Ga content.[19] Figure 1(a) displays the normalized PL spectra of all seven $CuIn_{1-x}Ga_xSe_2$ single crystals from which the gallium content was determined by the position of its maximum. Table I summarizes the samples' elemental composition determined by energy dispersive x-ray spectroscopy (EDX) and photoluminescence. The average of these quantities was rounded and used as the characteristic gallium content of each sample. Some samples were also analyzed by x-ray photoelectron spectroscopy (XPS) and Raman spectroscopy, which showed elemental compositions in agreement with the already determined by EDX and PL. Details of the XPS quantification and the Raman analysis can be found in Sec. S2 of the supplementary material.

Once the gallium content of each sample was determined, the Seebeck coefficient ($S = -\Delta V_{TH}/\Delta$), which measures the thermoelectric voltage V_{TH} generated as a response to an applied temperature difference ΔT, was measured in order to investigate the type of majority carrier. Negative values of S indicate that electrons are the majority carrier (N-type), and positive values indicate that conduction is carried by holes (P-type). The slope of the measured thermovoltages as a function of temperature gradients is equal to the Seebeck coefficient. Linear fits are presented in Fig. 1(b) for all investigated samples. These measurements confirmed the expected N-type character of the samples with the lowest gallium contents; however, a clear change in the thermoelectric behavior can be seen for gallium contents higher than 15%. First, the sign of the Seebeck coefficient changes from negative to positive (values listed in Table I), indicating that the majority carrier changes from electrons to holes (N to P transition). Furthermore, the magnitude of the Seebeck coefficient increases, which suggests that the Fermi level (E_F) has moved further away from the respective band edges since the Seebeck coefficient is defined in terms of the semiconductor energy levels as[20]

$$S_n = -\frac{k_B}{q}\left(\frac{5}{2} + r_e - \frac{E_F - E_C}{k_B T}\right),$$

$$S_p = \frac{k_B}{q}\left(\frac{5}{2} + r_h - \frac{E_V - E_F}{k_B T}\right).$$

For an N-type (S_n) and P-type (S_p) semiconductor, k_B is the Boltzmann constant, q is the elementary charge, $r_{e,h}$ is a term that depends

© Author(s) 2022

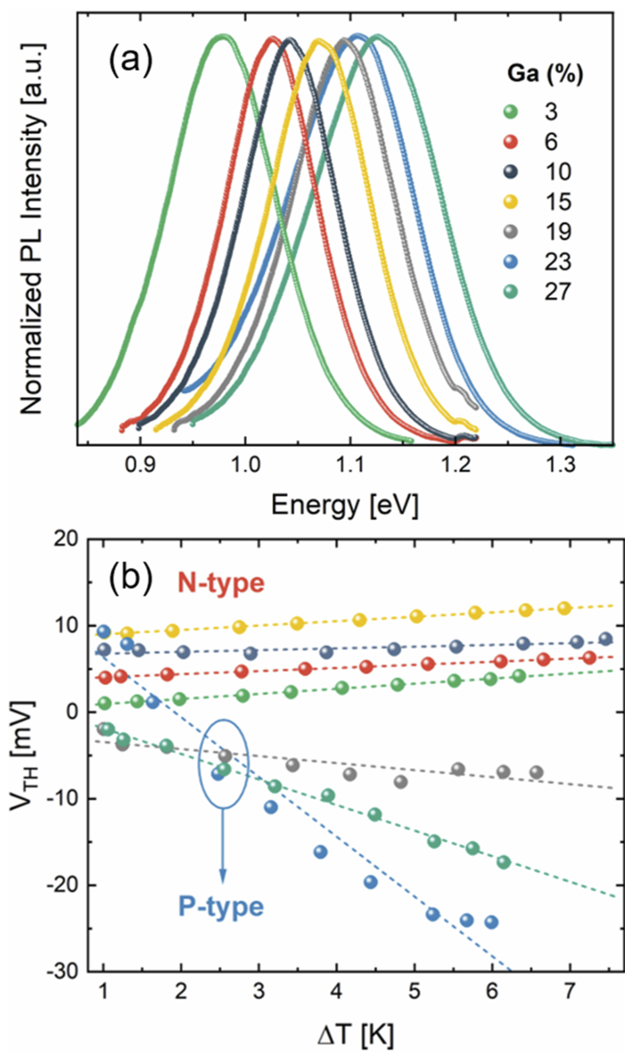

FIG. 1. Normalized photoluminescence spectra of all the $CuIn_{1-x}Ga_xSe_2$ samples showing the expected blue shift for higher gallium contents corresponding to the increase in bandgap (a). Seebeck coefficient determination (data shifted vertically for clarity) (b). The same color code applies to both figures.

on the carrier scattering mechanism, E_F is the Fermi level, and $E_{V,C}$ is the corresponding valence or conduction band energy. Values of the Seebeck coefficient for the strongly N-doped samples are in agreement with previous reports.[21]

In order to corroborate the apparent decrease in carrier concentration after the transition from N to P, an analysis of the electrical conductivity (σ) at room temperature and its temperature-dependency for selected samples was carried out, and the activation energy (E_A) was determined from the Arrhenius plot in Fig. 2(a). All the N-type samples analyzed were found to be more conducive and to have lower activation energy (41–76 meV) than the P-type ones (296–431 meV). Details on the determination of the activation energies can be found in Sec. S5 of the supplementary material. This difference in activation energy is probably due to the nature of the defects involved in the conductivity, first shallow donors and then deeper acceptors (as shallow acceptors are likely compensated). The low activation energy of the N-type samples, nonetheless, could partially be due to the influence of the thermally activated mobility, as activation energies in the range of 3–20 meV have been reported.[4] The measured increase in conductivity and activation energy supports the Seebeck coefficient trend of decreasing carrier concentration as the gallium content increases toward the N-to-P transition. In order to figure out whether the high activation energy was a characteristic of higher Ga contents only, a P-type sample with a 7% gallium content was also analyzed. To achieve this, a potassium fluoride post-deposition treatment (KF-PDT) was performed on the N-type absorber in order to change the conductivity type to P. The N-to-P type inversion was confirmed by the change in the Seebeck coefficient from −0.346 mV/K (N-type) to 0.671 mV/K (P-type) after the KF-PDT. The Seebeck coefficient measurements and more information regarding the type inversion caused by potassium in $CuInSe_2$ single crystals can be found in Ref. 22. It is worth mentioning that the reported Seebeck coefficient of −0.346 mV/K for the N-type sample is almost the same as the one reported herein for a 6% Ga (−0.36 mV/K). Despite the low Ga content, the activation energy of the P-type KF-treated sample was still considerably larger than the E_A of its N-type counterpart, suggesting that the high activation energies measured are actually a consequence of the majority charge carriers being holes (and their concentration) and not because of the increase in Ga content itself. A similar observation in pure $CuInSe_2$ has been reported when the N-to-P transition is caused by the copper content.[4]

TABLE I. Copper content, gallium percentage determined by different techniques, and Seebeck coefficient of all the $Cu(In,Ga)Se_2$ single crystals investigated.

Sample name	Cu/(In + Ga)	Ga % EDX 5 kV	Ga % PL	Ga % average	Ga % XPS	Seebeck coefficient (mV/K)
CIGSe298	0.86	5.2	0.0	3	⋯	−0.58 ± 0.01
CIGSe295	0.89	7.0	5.2	6	6.0	−0.35 ± 0.01
CIGSe296	0.89	10.4	8.8	10	10.0	−0.20 ± 0.04
CIGSe297	0.88	14.7	14.5	15	14.0	−0.50 ± 0.01
CIGSe299	0.88	19.5	18.8	19	20.0	0.80 ± 0.16
CIGSe304	0.83	24.0	21.6	23	⋯	6.90 ± 0.54
CIGSe305	0.82	29.2	25.2	27	⋯	2.95 ± 0.07

© Author(s) 2022

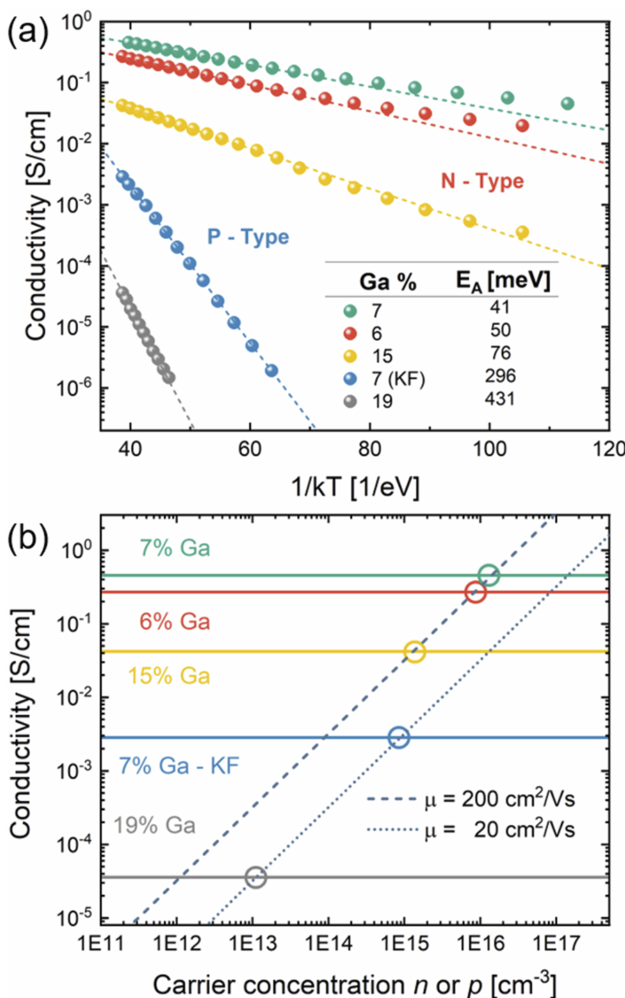

FIG. 2. Temperature-dependent conductivity measurements of N and P-type Cu(In,Ga)Se_2 single crystals (a). Best fits to the measured data are shown as dotted lines from which the activation energies were extracted. Determination of the carrier concentration from measured conductivity values for two different carrier mobilities (b).

From the measured conductivity values at room temperature and using $p(n) \gg n(p)$, we can estimate the carrier concentration as $p(n) = \sigma/q\mu_{h(e)}$, where q is the elementary charge and $\mu_{h(e)}$ is the hole (electron) mobility. Values of μ_e between 40 and 200 cm^2/V s measured by Hall have been reported for N-type $CuInSe_2$ single crystals grown by MOVPE with Cu contents ranging from 0.8 to 0.9,[4] while values of μ_h in close-to-stoichiometry $CuGaSe_2$ samples, between 20 and 150 cm^2/V s[1,23] Carrier mobility in both ternaries is strongly dependent on the Cu content, as it has been demonstrated to increase toward Cu-rich compositions.[4,24] Figure 2(b) shows the estimated carrier concentration for the same set of N and P-type samples for two different mobility values. By taking μ_e = 200 cm^2/V s, the carrier concentration of the N-type samples is estimated to be around 1.3×10^{15} to 1.4×10^{16} cm^{-3}; the P-type samples, on the other hand, are found to have carrier concentrations around two orders of magnitude lower for hole mobility of μ_h = 20 cm^2/V s. These electron and hole mobilities were chosen based on reported values for $CuInSe_2$ and $CuGaSe_2$ single crystals grown by MOVPE and with copper contents similar to the studied samples.[4,23] Indeed, reported carrier concentrations for N-type single crystals agree with our findings on the magnitude of n being in the order of the 10^{16} cm^{-3}.[4,25] Carrier concentration in $CuGaSe_2$, on the other hand, has been reported to drastically decrease from around 10^{16} to 10^{14} cm^{-3} below the stoichiometric point due to an increase in the degree of compensation,[23,26] in agreement with our estimated hole carrier concentrations of around 1.1×10^{13} to 8.9×10^{14} cm^{-3}.

As a way to confirm that the transition from N to P happens at gallium contents between 15% and 19%, x-ray photoelectron spectroscopy was used to analyze the change in the binding energy of the constituent elements. Since a considerable change in conductivity happens at the N-to-P transition, a shift in the binding energy would be expected due to the electrostatic difference in the interaction between specimen and spectrometer and surface charge accumulation.[27,28] Similarly, XPS has been used to study doping changes in moderately doped N and P-type silicon.[29] Figure 3 shows the Cu2p, In3d, Ga2p, and Se3d binding energies of samples with gallium contents close to the N-to-P transition region. As can be seen, a considerable difference in the binding energy of ~1.6 eV was measured in the sample containing 19% gallium with respect to the other samples with lower gallium contents. Since the shift was not only in one specific element but also in all the constituents, we attributed this to the change in conductivity due to the N-to-P transition rather than to a change in the chemical environment of a specific element.

So far, we have demonstrated that the conductivity type due to the addition of gallium to $CuInSe_2$ changes from N to P-type when the gallium content is between 15% and 19%, but we have not addressed the explanation behind this observation. The electronic structure of both $CuInSe_2$ and $CuGaSe_2$ ternary compounds is similar: at least two shallow acceptors (denoted as A1 and A2) located at 40 (A1) and 60 meV (A2) away from the valance band (VB) in $CuInSe_2$, and 60 (A1) and 100 meV (A2) in $CuGaSe_2$; and a shallow donor (D1) at 10 meV below the conduction band for both cases.[30,31] Theoretical studies[32–34] have assigned the origin of these electronic states to intrinsic point defects in the chalcopyrite crystal structure: A1 → Cu vacancies (V_{Cu}), A2 → Cu on an In/Ga site (Cu_{III}), and D1 → Cu interstitial (Cu_i) or In on a Cu site (In_{Cu}). For a more in-depth overview of defects in Cu(In,Ga)Se_2, the reader is referred to the review by Spindler *et al.*[31] Experimentally, neutron powder diffraction has been used to determine defect concentrations of alkali-free $CuInSe_2$, finding that the N-type character of Cu-poor samples is given by the shallow donor In_{Cu} substitutional defect,[35] which goes along with its theoretically calculated low formation energy[32,36].

The probability of the formation of defects depends on the chemical potential ($\Delta\mu$) of the constitutional elements, which, in turn, depends on the crystal growth conditions. In the work of Pohl and Albe, the formation energies of intrinsic point defects in both $CuInSe_2$ and $CuGaSe_2$ were calculated for different chemical potentials.[32] For selenium-poor, Cu, and In-rich conditions ($\Delta\mu_{In}$ = −0.2 eV and $\Delta\mu_{Cu}$ = 0 eV, point D in Fig. 1-up[32]), the intrinsic Fermi level in $CuInSe_2$ was found to be closer to the conduction

© Author(s) 2022

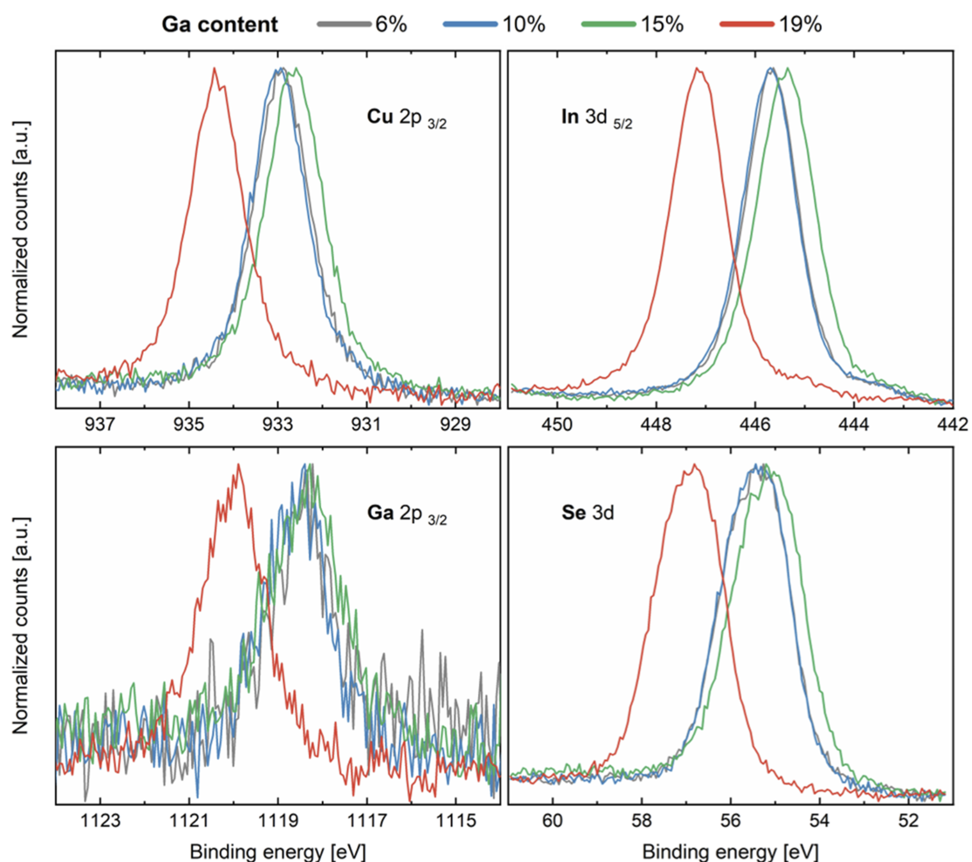

FIG. 3. Normalized Cu2p, In3d, Ga2p, and Se3d peaks of samples with different Ga contents around the critical gallium concentration of 15%–19%. The shift in binding energy is associated with the change in conductivity type from N-to-P.

band. On the contrary, under the same conditions (most Se poor point at $\Delta\mu_{Ga} = -0.3$ eV, point D in Fig. 1-down[32]), the intrinsic Fermi level in $CuGaSe_2$ was found to be below midgap. Thus, the theory also predicts an N-to-P transition due to the addition of Ga. Therefore, we analyzed the trends in formation energy of the previously described donors and acceptors in order to understand what happens at the critical gallium concentration of 15%–19%. The validity of this analysis resides in the fact that changes in the chemical potential would result in a shift of all formation energies but would not affect the observed trends.

Since the formation energy of defects depends on the position of the Fermi level, we first estimate E_F using the carrier concentrations previously obtained and literature values for the effective density of states[37] (details of the calculations can be found in Sec. S3 of the supplementary material). From this, we obtained that in the case of the N-type sample with 15% gallium, E_F is ~160 meV away from the CB, and in the case of the P-type sample with 19%, E_F is at 360 meV from the VB. Figure 4(b) shows the position of the calculated Fermi level for these and other selected samples. Based on this information, we proceeded to analyze the change in formation energies of A1, A2, and D1 in two situations: (A) from an N-type $CuInSe_2$ (E_F = 200 meV from CB) to an N-type $CuGaSe_2$ (E_F = 400 meV from CB) and (B) from an N-type $CuInSe_2$ (E_F = 200 meV from CB) to a P-type $CuGaSe_2$ (E_F = 400 meV from VB). The values of 200 and 400 meV were chosen, assuming that the carrier concentration would decrease further at the N-to-P transition region. A value of E_F = 200 meV away from the CB would indicate a carrier concentration of $n = 2.8 \times 10^{14}$ cm^{-3}, while a value of E_F = 400 meV away from the VB of $p = 2.6 \times 10^{12}$ cm^{-3}. The values of the formation energies were taken from Ref. 32, and the two cases are illustrated in Fig. 4(a) (more details in Sec. S4 of the supplementary material). By analyzing case A, it is possible to make the following deductions: With an increase of gallium, (I) the formation energy of both possible donors increases, (II) the formation energy of both acceptors decreases, and (III) the formation energy of A1 approaches zero. As a result, N-type $CuGaSe_2$ becomes very unlikely. For case B (which represents what has been experimentally observed), we observe the opposite trend. Interestingly, the defect with the lowest formation energy changes depending on the gallium content. For Ga/(Ga + In) < 0.5, the acceptor V_{Cu} dominates, but in higher gallium contents, the donor III_{Cu} has the lowest formation energy, which would go along with reports of Cu-poor $CuGaSe_2$ being strongly self-compensated.[38]

From the previous analysis, we can explain our experimental results as follows: When gallium is introduced to N-type $CuInSe_2$, the Fermi level starts to move away from the conduction band, because due to the lower formation energy of acceptor-type defects,

© Author(s) 2022

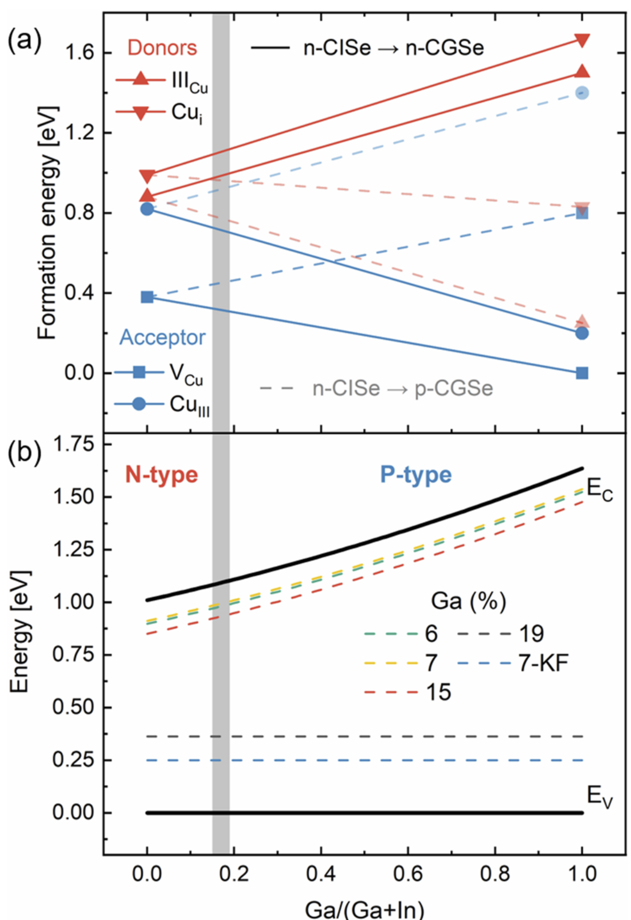

FIG. 4. Formation energy of the two possible donor defects III_{Cu} and Cu_i (red) and the two shallow acceptors A1 and A2 (blue). The points for $CuInSe_2$ correspond to a Fermi level 200 meV away from the conduction band (N-type) while two sets of points are displayed for $CuGaSe_2$, assuming an N-type (solid line) and a P-type (dotted line), in both cases, the Fermi level is assumed to be 400 meV away from the bands (a). All formation energies were taken from the work of Pohl and Albe.[32] Band diagram showing the calculated Fermi level for N and P-type samples with different gallium contents (b). The energy of the valance band is assumed constant and the bandgap calculated according to the equation given in the text.

more acceptors are formed. If the conductivity remained N-type (case A), further addition of gallium would result in the spontaneous formation of V_{Cu} (formation energy approaching zero), which would move the Fermi level below midgap, making the material P-type, which is always the case in $CuGaSe_2$. When the gallium content reaches the critical concentration of 15%–19%, as the formation of acceptor defects becomes more energetically favorable, the acceptor density (N_A) overpasses the donors (N_D), resulting in the material changing to P-type. In this situation (case B), further addition of gallium would result in an increased degree of compensation ($K = N_D/N_A$ for a P-type semiconductor) as the formation energy of donor-like defects decreases. As an unavoidable consequence of the increased degree of compensation, stronger electrostatic potential fluctuations would be expected as the gallium content increases. Experimental evidence of this can be found in literature, where the magnitude of these fluctuations (denoted as γ) in $CuGaSe_2$ was found to be greater than in $CuInSe_2$ for copper contents around 0.9 (γ_{CGSe} = 29–36 meV and γ_{CISe} = 15–28 meV).[39] Our own studies in stoichiometric alkali-free Cu(In,Ga)Se_2 single crystals[40] also support this implication as we have observed experimental evidence of higher Urbach energies caused by electrostatic potential fluctuations in Cu(In,Ga)Se_2 than in $CuInSe_2$.

IV. CONCLUSION

In summary, we studied the N-to-P transition in Cu-poor $CuInSe_2$ caused by the alloy with gallium. Our results demonstrated that Cu(In,Ga)Se_2 can be intrinsically grown as an N-type semiconductor as long as the gallium content is below the critical concentration of 15%–19%. The transition from N to P-type was confirmed by the change in the sample's thermoelectric behavior and the shift in binding energy measured by XPS. Furthermore, by measuring electrical conductivity and taking estimated mobility, we found that the carrier concentration has a decreasing trend toward the N-to-P transition region, dropping around two orders of magnitude (from $n \approx 1.3 \times 10^{15}$–$1.4 \times 10^{16}$ cm^{-3} to $p \approx 1.1 \times 10^{13}$–$8.9 \times 10^{14}$ cm^{-3}) when the material becomes P-type. By analyzing the trends in formation energy of donor and acceptor-like defects, we concluded that the N-to-P transition due to the addition of gallium is caused by (I) the more energetically favored formation of acceptor-like defects as the formation energy of acceptor states decreases and of donor states increases and (II) the fact that a Fermi level above midgap results in the instant formation of V_{Cu}, preventing N-type doping. With this work, we aimed at providing experimental evidence and addressing the long-standing discussion in the chalcopyrite community on the possibility to grow N-type Cu(In,Ga)Se_2.

SUPPLEMENTARY MATERIAL

See the supplementary material for the details on the heteroepitaxial growth, XPS, Raman spectroscopy, Fermi level calculations, and formation energies determination.

ACKNOWLEDGMENTS

This work was supported by the Luxembourgish Fond National de la Recherche in the framework of Project Nos. C17/MS/11696002 GRISC, PRIDE17/12246511/PACE, and 11244141 SUNSPOT. The authors thank Dr. Nathalie Valle and Brahime El Adib from the Luxembourg Institute of Science and Technology for all their support regarding the SIMS measurements. The authors also thank Dr. Florian Werner for his contribution to the conductivity measurements of selected samples and the fruitful discussions, as well as Thomas Schuler, Bernd Uder, and Ulrich Siegel for their technical support. For the purpose of open access, the authors have applied a Creative

© Author(s) 2022

Commons Attribution 4.0 International (CC BY 4.0) license to any Author Accepted Manuscript version arising from this submission.

AUTHOR DECLARATIONS

Conflict of Interest

The authors have no conflicts to disclose.

Author Contributions

Omar Ramírez: Conceptualization (equal); Data curation (equal); Formal analysis (equal); Investigation (equal); Methodology (equal); Visualization (equal); Writing – original draft (equal); Writing – review & editing (equal). **Evandro Martin Lanzoni:** Data curation (equal); Formal analysis (equal); Investigation (equal); Writing – original draft (equal). **Ricardo G. Poeira:** Data curation (equal); Formal analysis (equal); Investigation (equal); Writing – original draft (equal). **Thomas P. Weiss:** Conceptualization (equal); Methodology (equal). **Renaud Leturcq:** Data curation (equal); Formal analysis (equal); Investigation (equal); Validation (equal); Writing – original draft (equal). **Alex Redinger:** Funding acquisition (equal); Project administration (equal); Resources (equal); Validation (equal); Writing – original draft (equal). **Susanne Siebentritt:** Conceptualization (equal); Formal analysis (equal); Funding acquisition (equal); Investigation (equal); Methodology (equal); Project administration (equal); Resources (equal); Supervision (equal); Validation (equal); Writing – original draft (equal); Writing – review & editing (equal).

DATA AVAILABILITY

The data that support the findings of this study are openly available in Zenodo at https://doi.org/10.5281/zenodo.6362649, Ref. 41, as well as from the corresponding author upon reasonable request.

REFERENCES

[1] L. Mandel, R. Tomlinson, M. Hampshire, and H. Neumann, Solid State Commun. **32**, 201 (1979).
[2] H. Neumann and R. D. Tomlinson, Sol. Cells **28**, 301 (1990).
[3] J. Parkes, R. D. Tomlinson, and M. J. Hampshire, J. Cryst. Growth **20**, 315 (1973).
[4] F. Werner, D. Colombara, M. Melchiorre, N. Valle, B. El Adib, C. Spindler, and S. Siebentritt, J. Appl. Phys. **119**, 173103 (2016).
[5] D. J. Schroeder and A. A. Rockett, J. Appl. Phys. **82**, 4982 (1997).
[6] R. Noufi, R. Axton, C. Herrington, and S. K. Deb, Appl. Phys. Lett. **45**, 668 (1984).
[7] F. Babbe, H. Elanzeery, M. H. Wolter, K. Santhosh, and S. Siebentritt, J. Phys.: Condens. Matter **31**, 425702 (2019).
[8] C. Persson, Y.-J. Zhao, S. Lany, and A. Zunger, Phys. Rev. B **72**, 035211 (2005).
[9] Y.-J. Zhao, C. Persson, S. Lany, and A. Zunger, Appl. Phys. Lett. **85**, 5860 (2004).
[10] Ç. Kılıç and A. Zunger, Phys. Rev. B **68**, 075201 (2003).
[11] Y. Ren, Y. Hu, Z. Hu, and L. Xue, Res. Phys. **20**, 103774 (2021).
[12] M. Han, P. Deák, Z. Zeng, and T. Frauenheim, Phys. Rev. Appl. **15**, 044021 (2021).
[13] M. Rusu, S. Wiesner, R. Würz, S. Lehmann, S. Doka-Yamigno, A. Meeder, D. Fuertes Marrón, M. Bär, V. Koteski, H.-E. Mahnke, E. Arushanov, J. Beckmann, K. Höhn, W. Fritsch, W. Bohne, P. Schubert-Bischoff, M. Heuken, A. Jäger-Waldau, A. Rumberg, and T. Schedel-Niedrig, Sol. Energy Mater. Sol. Cells **95**, 1555 (2011).
[14] S. Thiru, M. Fujita, A. Kawaharazuka, and Y. Horikoshi, Appl. Phys. A **113**, 257 (2013).
[15] S. Ishizuka, Phys. Status Solidi A **216**, 1800873 (2019).
[16] S. B. Zhang, S.-H. Wei, and A. Zunger, Phys. Rev. Lett. **84**, 1232 (2000).
[17] P. Lunca-Popa, J. Afonso, P. Grysan, J. Crêpellière, R. Leturcq, and D. Lenoble, Sci. Rep. **8**, 7216 (2018).
[18] S.-H. Wei, S. B. Zhang, and A. Zunger, Appl. Phys. Lett. **72**, 3199 (1998).
[19] M. I. Alonso, M. Garriga, C. A. Durante Rincón, E. Hernández, and M. León, Appl. Phys. A **74**, 659 (2002).
[20] C. Herring, Phys. Rev. **96**, 1163 (1954).
[21] S. Endo, T. Irie, and H. Nakanishi, Sol. Cells **16**, 1 (1986).
[22] O. Ramírez, M. Bertrand, A. Debot, D. Siopa, N. Valle, J. Schmauch, M. Melchiorre, and S. Siebentritt, Sol. RRL **5**, 2000727 (2021).
[23] A. Gerhard, W. Harneit, S. Brehme, A. Bauknecht, U. Fiedeler, M. C. Lux-Steiner, and S. Siebentritt, Thin Solid Films **387**, 67 (2001).
[24] S. Siebentritt and S. Schuler, J. Phys. Chem. Solids **64**, 1621 (2003).
[25] S. M. Wasim, Sol. Cells **16**, 289 (1986).
[26] S. Siebentritt, L. Gütay, D. Regesch, Y. Aida, and V. Deprédurand, Sol. Energy Mater. Sol. Cells **119**, 18 (2013).
[27] D. R. Baer, K. Artyushkova, H. Cohen, C. D. Easton, M. Engelhard, T. R. Gengenbach, G. Greczynski, P. Mack, D. J. Morgan, and A. Roberts, J. Vac. Sci. Technol. A **38**, 031204 (2020).
[28] D. R. Baer, C. F. Windisch, Jr., M. H. Engelhard, and K. R. Zavadil, J. Surf. Anal. **9**, 396 (2002).
[29] H. Sezen and S. Suzer, J. Chem. Phys. **135**, 141102 (2011).
[30] S. Siebentritt, M. Igalson, C. Persson, and S. Lany, Prog. Photovoltaics **18**, 390 (2010).
[31] C. Spindler, F. Babbe, M. H. Wolter, F. Ehré, K. Santhosh, P. Hilgert, F. Werner, and S. Siebentritt, Phys. Rev. Mater. **3**, 090302 (2019).
[32] J. Pohl and K. Albe, Phys. Rev. B **87**, 245203 (2013).
[33] M. Malitckaya, H.-P. Komsa, V. Havu, and M. J. Puska, Adv. Electron. Mater. **3**, 1600353 (2017).
[34] L. E. Oikkonen, M. G. Ganchenkova, A. P. Seitsonen, and R. M. Nieminen, J. Phys.: Condens. Matter **26**, 345501 (2014).
[35] C. Stephan, S. Schorr, M. Tovar, and H.-W. Schock, Appl. Phys. Lett. **98**, 091906 (2011).
[36] J. Bekaert, R. Saniz, B. Partoens, and D. Lamoen, Phys. Chem. Chem. Phys. **16**, 22299 (2014).
[37] J. L. Gray, R. Schwartz, and Y. J. Lee, ECE Technical Reports, Purdue University, 1994, p. 173.
[38] S. Schuler, S. Siebentritt, S. Nishiwaki, N. Rega, J. Beckmann, S. Brehme, and M. C. Lux-Steiner, Phys. Rev. B **69**, 045210 (2004).
[39] S. Siebentritt, N. Papathanasiou, and M. C. Lux-Steiner, Physica B **376-377**, 831 (2006).
[40] O. Ramírez, J. Nishinaga, M. Melchiorre, and S. Siebentritt, "On the origin of tail states in $Cu(In,Ga)Se_2$" (unpublished).
[41] O. Ramírez, E. M. Lanzoni, R. G. Poeira, T. P. Weiss, R. Leturcq, A. Redinger, and S. Siebentritt (2022). "N to P in CIGSe," Zenodo.

© Author(s) 2022